Covalent Patterning and Rapid Visualization of Latent Fingerprints with Photo-Cross-Linkable Semiconductor Polymer Dots

Haobin Chen,[†] Kaiwen Chang,[†] Xiaoju Men,[†] Kai Sun,[†] Xiaofeng Fang,[†] Chi Ma,[†] Yongxi Zhao,[‡] Shengyan Yin,[†] Weiping Qin,[†] and Changfeng Wu*,[†]

[†]State Key Laboratory on Integrated Optoelectronics, College of Electronic Science and Engineering, Jilin University, 2699 Qianjin Street, Changchun, Jilin 130012, China

[‡]Key Laboratory of Biomedical Information Engineering of Education Ministry, School of Life Science and Technology, Xi'an Jiaotong University, Xi'an, Shanxi 710049, China

S *Supporting Information*

ABSTRACT: Fingerprint imaging and recognition represent the most important approach in personal identification. Here we designed and synthesized oxetane-functionalized semiconductor polymer dots (Ox-Pdots) for covalent patterning and rapid visualization of latent fingerprints. The high fluorescence brightness, large Stokes shift, and excellent surface properties of the Ox-Pdots lead to fingerprint imaging with high sensitivity and resolution. Fingerprint ridge structures with the first, second, and third levels of details were clearly developed within minutes. The method was facile and robust for visualization of fingerprints on various surfaces including glass, metal, and plastics. Moreover, the oxetane groups in the Ox-Pdots undergo cross-linking reactions induced by a short-time UV irradiation, yielding 3-D intermolecular polymer network. The resulting fingerprint patterns exhibit unparalleled stability against rigorous treatment, as compared to those by traditional Pdots. Our results demonstrate that the Ox-Pdots hold great promise for latent fingerprint imaging and fluorescence anticounterfeiting applications.

KEYWORDS: *semiconductor polymer, nanoparticle, fingerprint, fluorescence, patterning, anticounterfeiting*
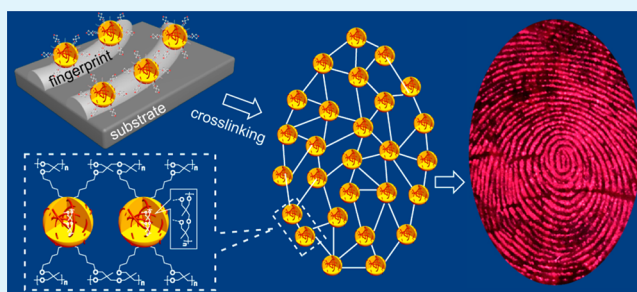
INTRODUCTION

When a finger comes into contact with the surface of an object, a complex mixture of natural secretions from the skin pores and external contaminants from the environment is transferred to the surface, generating a fingerprint. Because of the uniqueness and permanence of the friction ridge arrangements, fingerprints have become one of the most useful approaches for criminal identification since their early forensic applications in the 19th century. To date, the fingerprint is still the cornerstone of forensic evidence, and has also been widely used in areas such as individual credentials, access control, and bioanalysis.[1−3] In most cases, however, fingerprints are invisible because of their poor optical contrast to naked eyes, thus requiring physical or chemical treatment to enable visualization. During the past century, numerous methods and reagents, including powder dusting,[4] metal deposition,[5,6] cyanoacrylate/iodine fuming,[7,8] and fluorescence staining,[9] have been developed for detecting and visualizing latent fingerprints. Recently, methods based on biomolecular recognition have been demonstrated for both fingerprint visualization and detection of human metabolites with diagnostic or forensic values.[10−14]

Despite the various efforts and progress, there are a number of problems associated with the current methods for fingerprint development. For example, powder dusting, the most commonly used procedure, can cause inevitable destruction of the fingerprint details when brushing magnetic or fluorescent powders on latent fingerprints. Fingerprint images developed by iodine fuming fade away rapidly upon exposure to the air. In addition, the biolabeling methods typically involve complex preparation of nanoparticle bioconjugates.[15] Of great value in forensic investigations is the preservation time of material evidence. The important articles with fingerprints found in a crime scene should be handled and preserved with particular care for rigorous analysis. Forensic scientists particularly require that the fingerprints developed by diverse techniques maintain a good and robust pattern for a long preservation time.[16] Therefore, development of new materials and methods that can clearly visualize and permanently stabilize latent fingerprints in a facile, rapid, accurate, nondestructive, and effective manner is of considerable significance.

Here we demonstrate semiconductor polymer dots comprising side-chain oxetane groups for covalent patterning of latent fingerprints. Fluorescent Pdots have recently generated tremendous interest due to their superior properties such as

high brightness, excellent photostability, and biocompatibility for biological applications.[17−21] The high fluorescence brightness, large Stokes shift, and excellent surface properties of the Ox-Pdots in this work lead to great sensitivity and selectivity in fingerprint imaging. More importantly, the Ox-Pdots, once bound with the fingerprint ridges, undergo photo-cross-linking reactions under a UV irradiation. The resulting image patterns show unparalleled stability against rigorous treatments, indicating their great potential for fingerprint development and anticounterfeiting applications.

■ EXPERIMENTAL SECTION

Materials. 3-Methyl-3-oxetanemethanol, 1,6-dibromohexane, (4,4,5,5-tetramethyl-1,3,2-dioxaborolan-2-yl)benzene, bromobenzene, 2,7-dibromofluorene, and chloroform-d were obtained from J&K Chemical Ltd. 4,7-Dibromobenzo[c]-1,2,5-thiadiazole, 9,9-dioctyl-9H-fluorene-2,7-diboronic acid bis(pinacol) ester, 2,7-bis(4,4,5,5-tetramethyl-1,3,2-dioxaborolan-2-yl)-9,9-di-n-octylfluorene, and 4,7-bis(2-bromo-5-thienyl)-2,1,3-benzothiadiazole were obtained from Derthon Optoelectronic Materials Science & Technology Co., Ltd. Poly-(styrene-co-maleic anhydride) (PSMA, M_n = 1700), tetrakis-(triphenylphosphine)palladium(0) (Pd[PPh$_3$]$_4$, 99%), and triarylsulfonium hexafluorophosphate salts were purchased from Sigma-Aldrich. Blue-emitting semiconductor polymer poly(9,9-dihexylfluorenyl-2,7-diyl) (PDHF, M_w = 55 000, PDI = 2.7) and green-emitting semiconductor polymer poly[(9,9-dioctylfluorenyl-2,7-diyl)-co-10%(1,4-benzo-{2,1′,3}-thiadiazole)] (PF10BT, M_w = 15 000, PDI = 3.0) were purchased from American Dye Source, Inc. Red-emitting semiconductor polymer poly(9,9-dioctylfluorene)-co-5%(4,7-di-2-thienyl-2,1,3-benzothiadiazole) (PF5DTBT) was synthesized on the basis of the procedure described in a previous report.[22] All chemicals were used without further purification.

Characterization Methods. UV−vis absorption spectra were recorded on a Shimadzu UV-2550 spectrophotometer. Fluorescence emission spectra were measured on a Hitachi F-4500 fluorometer. The particle diameter distributions and zeta potential of the Pdots were determined by dynamic light scattering (DLS) with a Malvern Zetasizer Nano ZS instrument. The Pdot size and morphology were investigated by a Hitachi H-600 transmission electron microscope (TEM). Fourier transform infrared (FTIR) spectra were collected on a Nicolet 6700 FTIR spectrophotometer. The molecular weights of polymers were measured by the GPC method (515HPLC pump, Waters, 2414 refractive index detector). ^{1}H NMR spectra were obtained on a 300 MHz Varian Mercury. ^{13}C NMR spectra were obtained on a 500 MHz Bruker Avance.

Preparation of 3-[(6-Bromohexyloxy)methyl]-3-methyloxetane (3). In a 250 mL flask, to a solution of NaOH in deionized water (50 mL, 0.65 g/mL) were added 3-methyl-3-oxetanemethanol (1) (5.0 g, 0.049 mol), 1,6-dibromohexane (2) (35.9 g, 0.147 mol), tetrabutyl ammonium bromide (Bu$_4$NBr, 0.2 g, 0.62 mmol), and n-hexane (40 mL). The mixture was stirred at room temperature for 24 h and then refluxed for 2 h. After the solution was cooled to room temperature, deionized water (50 mL) was added to the solution. The solution was extracted with n-hexane (50 mL × 3) and deionized water (50 mL × 3). The combined organic layer was dried over MgSO$_4$. The solution was then concentrated, and the solvent was removed by rotary evaporation; the final product was obtained as a colorless liquid (10.1 g, 78%) after being purified by dry column chromatography on silica gel (ethyl acetate/n-hexane = 1/10 as eluent). ^{1}H NMR (300 MHz, CDCl$_3$, δ): 4.51 (d, 2H, J = 5.7 Hz), 4.35 (d, 2H, J = 5.7 Hz), 3.47 (t, 2H, J = 6.4 Hz), 3.46 (s, 2H), 3.41 (t, 2H, J = 6.9 Hz), 1.91−1.82 (m, 2H), 1.65−1.56 (m, 2H), 1.51−1.35 (m, 4H), 1.31 (s, 3H). ^{13}C NMR (150 MHz, CDCl$_3$): δ 79.93, 75.86, 71.11, 39.70, 33.59, 32.52, 29.16, 27.74, 25.15, 21.19.

Preparation of 9,9-Di-{3-[(3-methyloxetan-3-yl)methoxy]-hexyl)-2,7-dibromofluorene (5). In a 250 mL flask, to a solution of NaOH in deionized water (15 mL, 1.0 g/mL) were added 2,7-dibromofluorene (4) (1.3 g, 4 mmol), Bu$_4$NBr (0.165 g, 0.51 mmol), and dimethyl sulfoxide (DMSO, 35 mL). The mixture was stirred at 60

°C for 5 min, and then 3-[(6-bromohexyloxy)methyl]-3-methyloxetane (3) (2.3 g, 8.8 mmol) in DMSO (15 mL) was added; the mixture then refluxed for 12 h. After the solution was cooled to room temperature, the combined organic phases were washed with deionized water (75 mL × 3) and extracted with ethyl acetate (40 mL × 3) and deionized water (50 mL). The combined organic layer was dried (MgSO$_4$) and evaporated; the final product was obtained as a colorless thick solid (2.2 g, 79%) after being purified by dry column chromatography on silica gel (ethyl acetate/n-hexane = 1/5 as eluent). Mp: 63.2−64.0 °C. ^{1}H NMR (300 MHz, CDCl$_3$, δ): 7.53−7.45 (q, 6H), 4.45 (d, 4H, J = 5.7 Hz), 4.32 (d, 4H, J = 5.7 Hz), 3.40 (s, 4H), 3.33 (t, 4H, J = 6.6 Hz), 1.94−1.88 (m, 4H), 1.43−1.34 (m, 4H), 1.26 (s, 6H), 1.15−1.05 (m, 8H), 0.63−0.50 (m, 4H). ^{13}C NMR (150 MHz, CDCl$_3$): δ 152.33, 139.02, 130.18, 126.06, 121.45, 121.14, 80.16, 75.97, 71.43, 55.57, 40.08, 39.82, 29.60, 29.33, 25.68, 23.53, 21.33.

Synthesis of do-PFO Polymer. In a 50 mL flask, 9,9-di-{3-[(3-methyloxetan-3-yl)methoxy]hexyl}-2,7-dibromofluorene (5) (346.3 mg, 0.5 mmol) and monomer 9,9-dioctyl-9H-fluorene-2,7-diboronic acid bis(pinacol) ester (8) (321.3 mg, 0.5 mmol) were dissolved in toluene (10 mL); Bu$_4$NBr (6.4 mg, 0.02 mmol) and Na$_2$CO$_3$ (6 mL, 2 M) were also added. The reactants were stirred at room temperature, and the flask was degassed and recharged with nitrogen (repeated 6 times) before and after addition of Pd(PPh$_3$)$_4$ (10 mg, 0.008 mmol) to the mixture. The mixed solution was stirred at 90 °C for 2 days under N$_2$ atmosphere, and then (4,4,5,5-tetramethyl-1,3,2-dioxaborolan-2-yl)benzene (30 mg) dissolved in toluene (1 mL) was introduced to remove bromine end groups. After 5 h, bromobenzene (0.3 mL) was added to remove boronic ester end groups and further stirred for 6 h. After the mixture was cooled to room temperature, it was poured into methanol (100 mL). The precipitated solid was filtered and washed by ammonia solution, deionized water, ethanol, and acetone. The crude products were dissolved in tetrahydrofuran (THF, 15 mL), filtered by using 0.22 μm membrane, and reprecipitated in methanol (100 mL). The precipitate was then redispersed in acetone (150 mL) and stirred for 24 h. The resulting polymer was collected by filtration, and then dried at 40 °C under vacuum for 2 days, finally resulting in pale yellowish green solid (374.0 mg, 81%). ^{1}H NMR (300 MHz, CDCl$_3$, δ): 7.96−7.80 (m, 4H), 7.77−7.52 (m, 8H), 4.46 (d, 4H, J = 5.7 Hz), 4.32 (d, 4H, J = 5.7 Hz), 3.40 (s, 4H), 3.34 (t, 4H, J = 6.6 Hz), 2.25−1.98 (m, 8H), 1.62−1.35 (m, 4H), 1.26 (s, 6H), 1.23−1.01 (m, 30H), 0.83 (m, 12H) (Supporting Information Figure S1). Molecular weight was measured by GPC as M_n = 25 692, M_w = 64 360, PDI = 2.50.

Synthesis of do-PF10BT Polymer. In a 50 mL flask, 9,9-di-{3-[(3-methyloxetan-3-yl)methoxy]hexyl)-2,7-dibromofluorene (5) (277.0 mg, 0.4 mmol), monomer 4,7-dibromobenzo[c]-1,2,5-thiadiazole (7) (29.4 mg, 0.1 mmol), and monomer 9,9-dioctyl-9H-fluorene-2,7-diboronic acid bis(pinacol) ester (8) (321.3 mg, 0.5 mmol) were dissolved in toluene (10 mL); Bu$_4$NBr (6.4 mg, 0.02 mmol) and Na$_2$CO$_3$ (6 mL, 2 M) were also added. The following reaction conditions and purification procedure were similar to the synthesis of do-PFO polymer, finally resulting in bright yellow solid (286.5 mg, 68%). ^{1}H NMR (300 MHz, CDCl$_3$, δ): δ 8.12−7.37 (m, 14H), 4.46 (d, 4H, J = 5.7 Hz), 4.31(d, 4H, J = 5.7 Hz), 3.40 (s, 4H), 3.33 (t, 4H, J = 6.3 Hz), 2.27−2.03 (m, 8H), 1.51−1.34 (m, 4H), 1.26 (s, 6H), 1.23−1.03 (m, 30H), 0.83 (m, 12H). Molecular weight was measured by GPC as M_n = 9353, M_w = 17 495, PDI = 1.87.

Synthesis of do-PF5DTBT Polymer. In a 50 mL flask, 9,9-di-{3-[(3-methyloxetan-3-yl)methoxy]hexyl)-2,7-dibromofluorene (5) (311.7 mg, 0.45 mmol), monomer 4,7-bis(2-bromo-5-thienyl)-2,1,3-benzothiadiazole (6) (22.9 mg, 0.05 mmol), and monomer 9,9-dioctyl-9H-fluorene-2,7-diboronic acid bis(pinacol) ester (8) (321.3 mg, 0.5 mmol) were dissolved in toluene (10 mL); Bu$_4$NBr (6.4 mg, 0.02 mmol) and Na$_2$CO$_3$ (6 mL, 2 M) were also added. The following reaction conditions and purification procedure were similar to the synthesis of do-PFO polymer, finally resulting in dark red solid (319.2 mg, 71%). ^{1}H NMR (300 MHz, CDCl$_3$, δ): δ = 7.90−7.56 (m, 14H), 7.46−7.38 (m, 4H), 4.45 (d, 4H, J = 5.7 Hz), 4.31 (d, 4H, J = 5.7 Hz), 3.39 (s, 4H), 3.34 (t, 4H, J = 6.6 Hz), 2.29−1.96 (m, 8H), 1.66−1.34 (m, 4H), 1.25 (s, 6H), 1.23−1.05 (m, 32H), 0.82 (m,12H). Molecular

Scheme 1. Synthetic Route and Chemical Structures of the Photo-Cross-Linkable Semiconducting Polymers with Side-Chain Oxetane Groups
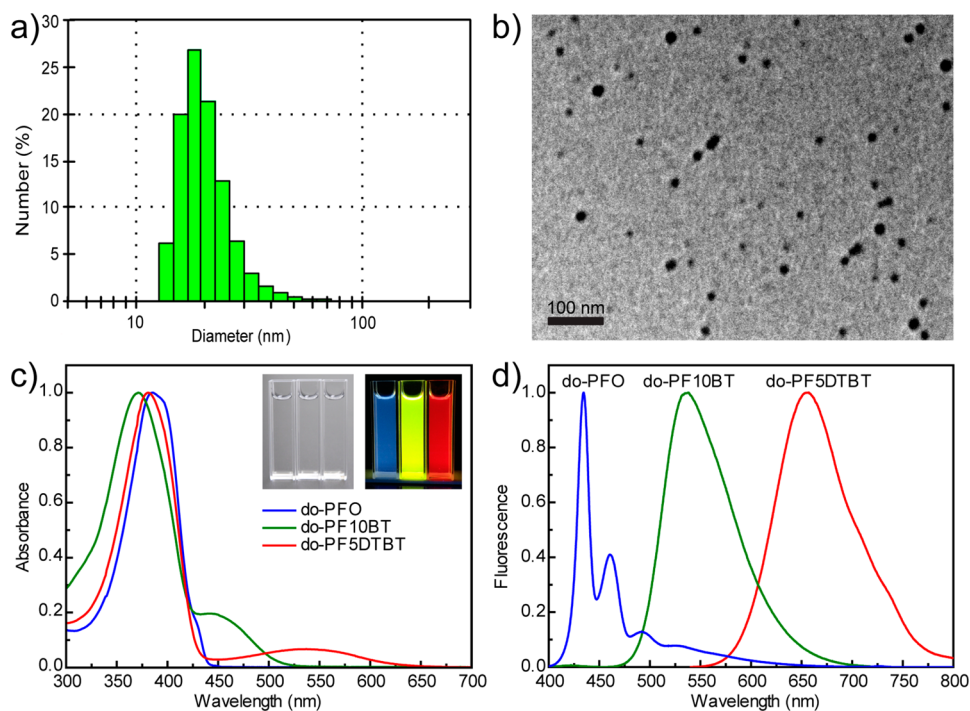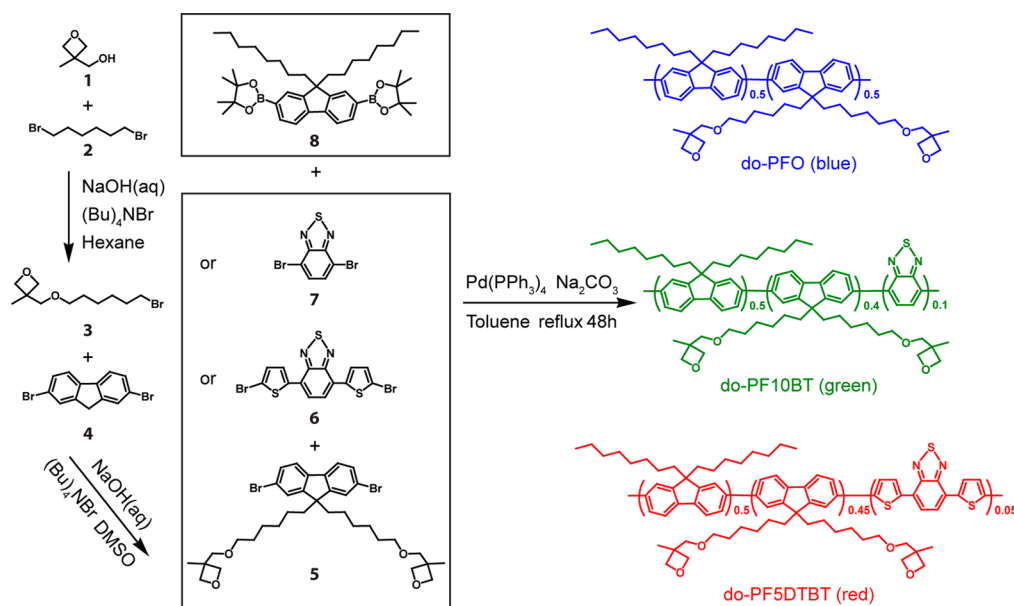

Figure 1. Characterizations of the Ox-Pdots. (a) Size distribution of do-PF10BT Pdots determined by DLS. (b) TEM image of do-PF10BT Pdots. (c) UV−vis absorption spectra of the Ox-Pdot solutions. The inset shows the Ox-Pdot solutions under daylight (left) and UV light illumination (right). (d) Emission spectra of the Ox-Pdot solutions.

weight was measured by GPC as M_n = 14 284, M_w = 30 498, PDI = 2.13.

Preparation of Pdots. The Pdots were prepared according to the nanoprecipitation method described previously.[23] In a typical preparation, 500 μg of a conjugated polymer and 50 μg of PSMA were completely dissolved in 10 mL of THF. A 3 mL portion of the polymer/THF solution was quickly dispersed into 10 mL of ultrapure water under vigorous sonication. The THF was then removed by nitrogen bubbling on a hot plate. A small fraction of aggregates was removed by filtration through a 0.22 μm membrane filter.

Fingerprints Development. Volunteers were asked to gently rub their fingertips over their forehead and nose region and then press on substrates (glass microscope slide, aluminum foil, iron spoon, and plastic Petridish) with minimal pressure. The area around each latent fingerprint was marked by a hydrophobic pen to keep the Pdots solution over the surface containing the fingerprints. Then, 0.5 mL of Pdot solution (500 μg/mL) was added on the substrate and incubated with the fingerprints for a certain time (1−5 min) at room temperature. For photo-cross-linking, the resulting sample was immersed in a water solution of photoinitiator (triarylsulfonium hexafluorophosphate salts, 3 wt %), and irradiated with a UV lamp

Scheme 2. Schematic Illustration for Visualization and Covalent Patterning of Latent Fingerprints with Photo-Cross-Linkable Ox-Pdots
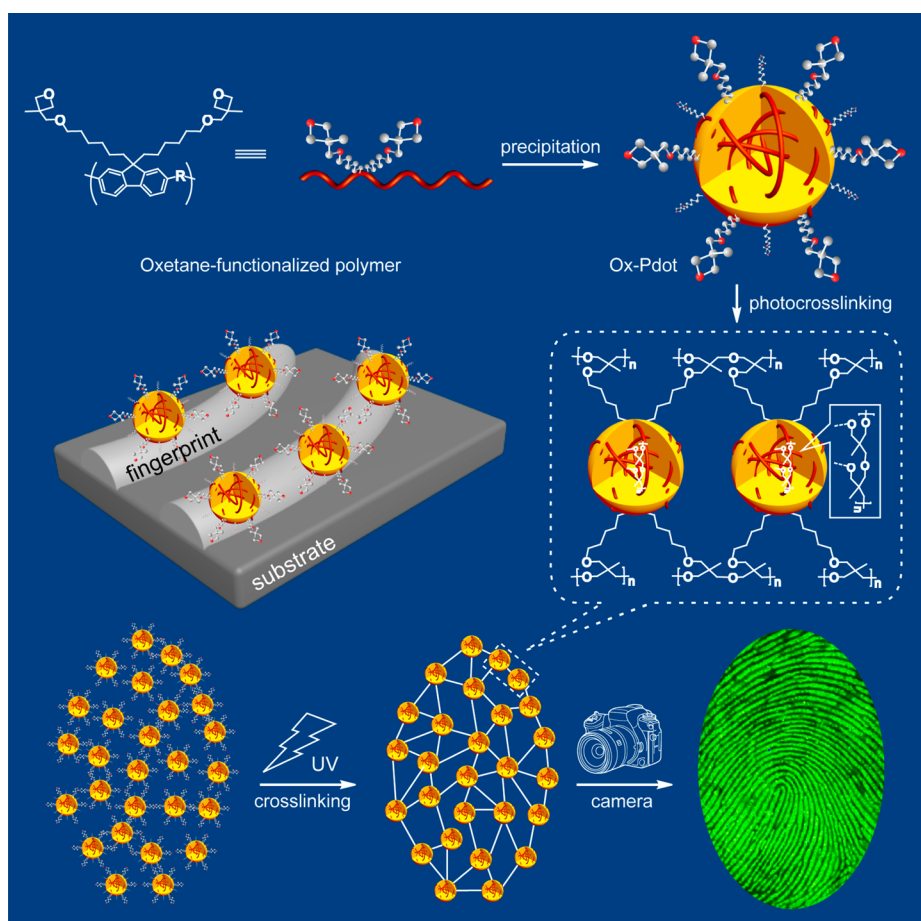
(high-pressure mercury lamp, 250 W) for 10 s at room temperature. The final sample was rinsed three times with ultrapure water and photographed by using a camera under a UV (~365 nm) lamp illumination.

■ RESULTS AND DISCUSSION

Synthesis and Characterization of Photo-Cross-Linkable Pdots. We choose polyfluorene-based backbone structures to synthesize oxetane-functionalized polymers because they exhibit great properties for the development of multicolor semiconducting polymers. Scheme 1 shows the synthetic routes of multicolor photo-cross-linkable polymers and related monomers. Oxetanes are commonly reactive functional groups for cationic photopolymerization, and they react with each other upon UV light irradiation. We first synthesize the fluorene monomer consisting of two oxetane functional groups in the side-chains, which was further copolymerized with the general fluorene monomer and a low band gap monomer (4,7-dibromobenzo[c]-1,2,5-thiadiazole or 4,7-bis(2-bromo-5-thienyl)-2,1,3-benzothiadiazole). Detailed synthesis procedures of the monomers and polymers were described in the Experimental Section. The three types of oxetane-functionalized semiconductor polymers are blue-emitting do-PFO polymer, green-emitting do-PF10BT polymer, and red-emitting do-PF5DTBT polymer, respectively. ^{1}H NMR (CDCl$_3$) measurements clearly indicate the presence of oxetane groups in the as-synthesized semiconductor polymers

(δ = 4.32 and δ = 4.46, 4H, two $-$CH$_2-$ in the oxetane ring, Supporting Information Figure S1).

To achieve great colloidal stability, we prepared the Pdots by using PSMA as a functional polymer.[24] The resulting Ox-Pdots have great colloidal stability: the aqueous suspensions are clear for months with no sign of aggregation. The particle diameters and morphology of Ox-Pdots were characterized by DLS (Figure 1a) and TEM (Figure 1b) measurements. For example, do-PF10BT Pdots exhibit a spherical morphology with an average diameter of ~18 nm (Figure 1a). The other two types of Ox-Pdots show similar morphology and particle sizes (Supporting Information Figure S2). All the Ox-Pdots show major absorption bands in the UV region (Figure 1c). With an UV excitation at 365 nm, the three types of Ox-Pdots exhibit intense emissions at three different colors (Figure 1d). Fluorescence quantum yields of the Ox-Pdots were determined to be 0.25 for do-PFO, 0.36 for do-PF10BT, and 0.20 for do-PF5DTBT, respectively. The dominant UV absorption, large Stokes shift, and high fluorescence quantum yields of the Ox-Pdots are promising for visualizing latent fingerprints.

Development and Covalent Patterning of Latent Fingerprints. Inorganic quantum dots (Qdots), including CdS,[25] CdSe,[26,27] and CdTe,[16,28] have been explored for latent fingerprint development. In previous studies we have demonstrated Pdots are 30 times brighter than Qdots of comparable size.[29] On the basis of the high brightness, nontoxicity, and photo-cross-linking properties of Ox-Pdots, we intended to explore their application for latent fingerprint
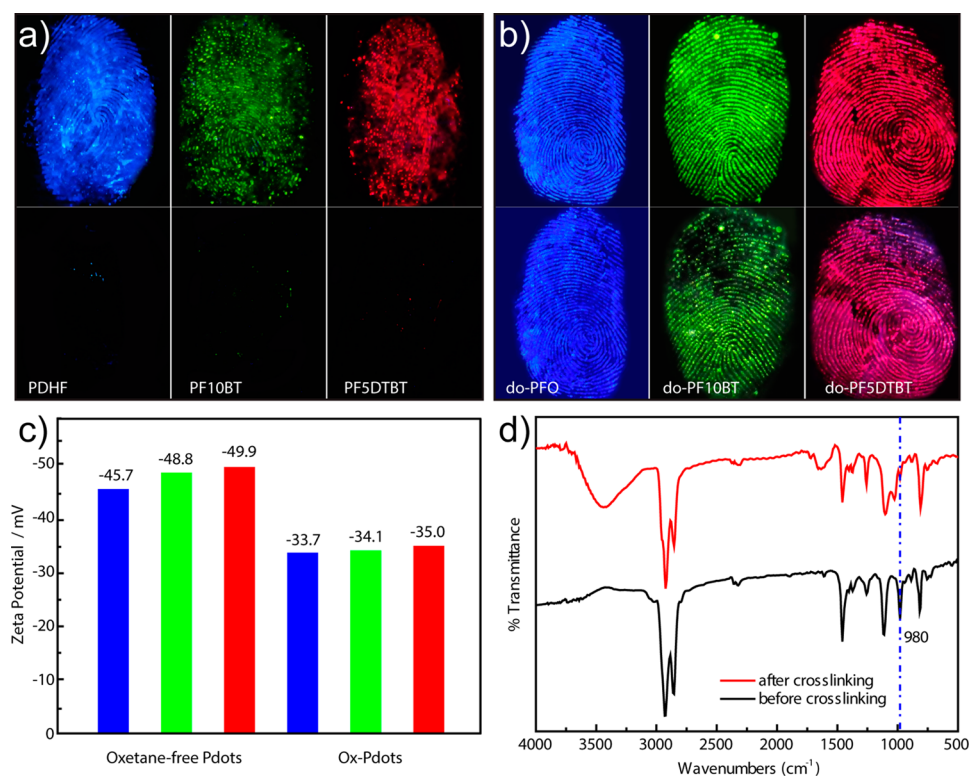
Figure 2. Fluorescence images of latent fingerprints developed with (a) traditional oxetane-free Pdots and (b) photo-cross-linkable Ox-Pdots. The top panel shows the high-quality fingerprint images developed by Ox-Pdots as compared to those by oxetane-free Pdots. The bottom panel shows the respective images after THF treatment. The fingerprint patterns by Ox-Pdots after photo-cross-linking are extremely stable against long-term THF treatment (24 h). In contrast, all the fingerprint patterns by oxetane-free Pdots are destroyed in THF for a short period of time (10 min). (c) Zeta potentials of traditional oxetane-free Pdots and photo-cross-linkable Ox-Pdots. (d) FTIR spectra of do-PFO before and after cross-linking.

imaging. Conventional Pdots without side-chain oxetane groups were also employed for comparative studies. Sebaceous fingerprints in our experiments were donated by volunteers who gently rubbed their fingertips over forehead and noses tamped them on different substrates with a minimal pressure. The substrates were incubated with different Pdots, and rinsed with ultrapure water, and then photographed with an ordinary camera under a UV lamp illumination (Scheme 2).

Figure 2 displays true-color fluorescence images of the fingerprints developed by traditional Pdots and photo-cross-linkable Pdots, respectively. By using the same Pdot concentration (500 μg/mL) and incubation time (2 min), all the Ox-Pdots yield much better and reproducible imaging quality (Figure 2b), while the conventional oxetane-free Pdots give poor resolution (Figure 2a). This distinctive observation highlights the importance of side-chain oxetane groups for developing well-resolved fingerprint structures. It is apparent that the interactions of Ox-Pdots with the fingerprint ridges are determined by their surface properties. As revealed by zeta potential measurements (Figure 2c), the Ox-Pdots show negative surface potentials around −35 mV, somewhat lower those of the oxetane-free Pdots (<−45 mV). We speculate that hydrophobic interactions should play an important role in the interactions between the Ox-Pdots and fingerprint residue, although electrostatic interactions can also contribute. As the density of oxetane side-chain groups is quite high (∼50% in monomer ratio), they are uniformly distributed on the Pdot surface. The chemical components of fingerprints include inorganic salts such as iron and sodium, amino acids, and lipids such as fatty acids, wax esters, squalene, and cholesterol.[30] It is

likely that the high-density ether groups of the Ox-Pdots preferentially interact with fatty residues of the fingerprint ridges, resulting in rapid and high-quality imaging of the latent fingerprints. It is worth noting that well-resolved fingerprint structures were developed by the Ox-Pdots within a couple of minutes. Such a rapid visualization may be practically helpful for screening potential crime scenes and capturing fingerprint clues.

A significant feature of the Ox-Pdots is that the developed fingerprint patterns can be covalently cross-linked to produce robust and long-lasting structures. The fingerprint patterns were irradiated with a UV lamp (high-pressure mercury lamp, 250 W) for 10 s in the presence of triarylsulfonium hexafluorophosphate salts as a photoinitiator that can induce the cross-linking reaction via a cationic ring-opening polymerization. As shown by the bottom images in Figure 2a,b, the fingerprint patterns after photo-cross-linking are extremely stable against rigorous treatment in organic solvent such as THF. Almost all the detailed structures remain with little changes after THF treatment for 24 h. In contrast, all the fingerprint patterns by the traditional Pdots are destroyed in THF in a short period of time (10 min). Fourier-transform infrared (FTIR) spectroscopy was performed to confirm the light-induced cross-linking behavior in the Ox-Pdots. Previous study demonstrated that oxetane groups could no longer be detected by FTIR after the photo-cross-linking reaction.[31] As shown by the FTIR spectra of do-PFO polymer (Figure 2d), the absorption band at 980 cm^{-1} is attributable to the cyclic ether linkage of the oxetane ring.[32] The characteristic band of oxetane ring disappeared after UV irradiation, accompanied by

the presence of some new bands around 1010−1130 cm^{-1} due to the acyclic ether linkage of the resultant polyether chains. These spectroscopic features indicate the occurrence of photo-cross-linking reactions in the Ox-Pdots. Taken together, these results indicate that the photo-cross-linkable Pdots are superior materials for covalently patterning latent fingerprints with high stability and long-term durability.

High-Resolution Imaging of Latent Fingerprints. The Ox-Pdots provide high sensitivity and reliability in latent fingerprint imaging. There are two main categories of fingerprint matching techniques that are used for fingerprint identification. The most widely used recognition technique, the minutiae-based method, first finds minutiae points and, after that, maps their relative placement on the finger to match ridge characteristics. Alternatively, pattern matching compares two images to see how similar they are. Useful protocols and flowcharts have been published as step-by-step descriptions of the comparative identification process. The examination method of ACE-V (analysis, comparison, evaluation, and verification) is the established methodology for perceiving minutiae in two fingerprints and making decisions. In all cases, the fingerprint image must provide a certain number of ridge details to give a powerful identification. A way to describe the fingerprint features by using three levels of details was introduced by David Ashbaugh.[33] Level 1 detail of friction ridge features describes the general overall direction of ridge flow in the fingerprint. Traditionally, the general pattern formed on the fingertips has been classified into generic classes. In the most widespread Henry system of classification, there are three essential fingerprint patterns: loop, whorl, and arch, which constitute 60−65%, 30−35% and 5% of all fingerprints, respectively.

Figure 3 shows fluorescence images that clearly indicate these three basic fingerprint patterns developed with Ox-Pdots. It is
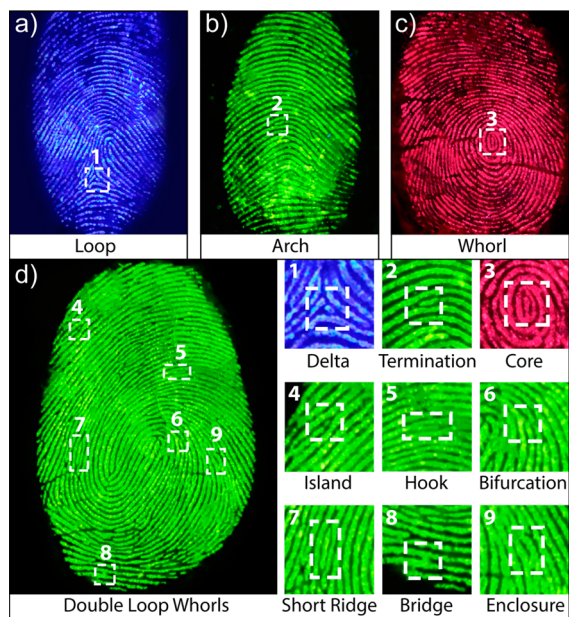
Figure 3. High-resolution fluorescence images of latent fingerprints. The images indicate four different fingerprint patterns including (a) loop, (b) arch, (c) whorl, and (d) double loop whorls. The magnified images show specific details, such as (1) delta, (2) termination, (3) core, (4) island, (5) hook, (6) bifurcation, (7) short ridge, (8) bridge, and (9) enclosure.

not sufficient for individualization but can be used for exclusion. Level 2 detail describes the specific ridge path, including the starting position, length, and end point of the ridge. Level 2 detail enables individualization. It is the relationship of these features across the print that defines the uniqueness of the fingerprint. Level 3 detail includes all attributes of a ridge, such as the edge shape, width, pores, and other permanent minutiae. The left image in Figure 3d displays a well-resolved ridge flow and pattern structure (level 1). Moreover, a number of magnified images of this fingerprint were shown in the right side of Figure 3d, which clearly illustrate Level 2 characteristics of the patterns, such as delta, core, termination, bifurcation, hook, island, short ridge, bridge, and enclosure. These detailed characteristics identified in the fingerprint form the basis of personal identification. We compared the fingerprint image developed by the Ox-Pdots with that captured with a blue inkpad to further confirm the accuracy of fingerprint imaging. As marked by the numbers in Figure 4, many identical minutia
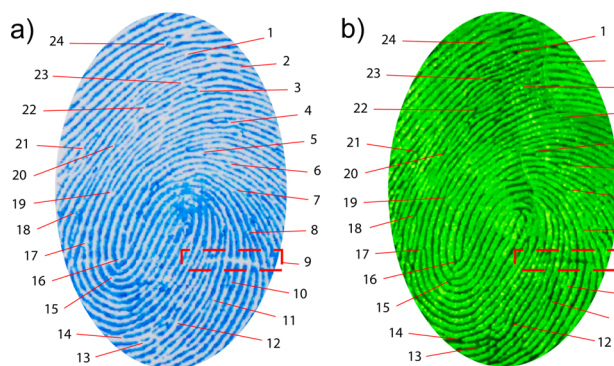
Figure 4. Comparison of the latent fingerprint stained by (a) a blue inkpad and (b) do-PF10BT Pdots. The numbers marked the identical minutia points simultaneously present in both of the two images, indicating the high-resolution development of the fingerprints by using the Ox-Pdots.

points were simultaneously observed in the blue image captured by inkpad (Figure 4a) and the fluorescent image developed by the Ox-Pdots (Figure 4b). Level 3 details such as ridge path deviation (point 24), width, shape, edge contour, and creases (point 9) could be clearly identified. These details can apparently lead to individualization, and they are also potentially useful in the identification of partial or damaged fingerprints. Overall, successful identification of the detailed substructures indicates the high sensitivity and reliability of the Ox-Pdots for rapid fingerprint development.

To demonstrate the practical usefulness, the Ox-Pdots were employed for developing fingerprints of different people on various substrates. Sebaceous fingerprints on different substrates, including glass slide, aluminum foil, iron spoon, and plastic Petri dish and polyvinyl difluoride (PVDF) membrane were incubated with do-PF10BT Pdots (Supporting Information Figure S3). Under a UV excitation, the images on these substrates exhibit bright fluorescent patterns, in which the details of fingerprint ridges could be clearly recognized. On the other hand, the fingerprints deposited on plastic substrates present a bit poorer resolution and higher background noise, indicating the substrate surface also affects the interaction of Ox-Pdots with the fingerprints. This fact is consistent with the hypothesis that hydrophobic interactions play a major role in the fingerprint development. We further demonstrate the
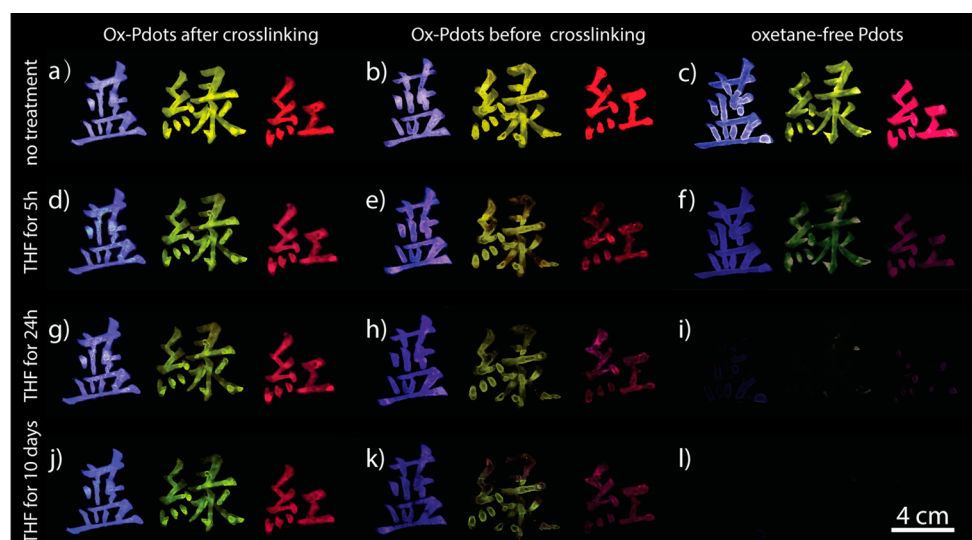
Figure 5. Stability of the handwritten patterns against THF treatment: (a) Ox-Pdots after cross-linking with no treatment; (b) Ox-Pdots before cross-linking with no treatment; (c) oxetane-free Pdots with no treatment; (d) Ox-Pdots after cross-linking in THF for 5 h; (e) Ox-Pdots before cross-linking in THF for 5 h; (f) oxetane-free Pdots in THF for 5 h; (g) Ox-Pdots after cross-linking in THF for 24 h; (h) Ox-Pdots before cross-linking in THF for 24 h; (i) oxetane-free Pdots in THF for 24 h; (j) Ox-Pdots after cross-linking in THF for 10 days; (k) Ox-Pdots before cross-linking in THF for 10 days; (l) oxetane-free Pdots in THF for 10 days;.

applications of the multicolor Ox-Pdots for detecting fingerprints from different people. As shown in Supporting Information Figure S4, all the Ox-Pdots developed fingerprints from nine volunteers displayed sufficient details of their ridge pattern structures. Again, these observations clearly indicate that the Ox-Pdots hold promise as a general approach for imaging latent fingerprints.

Besides the development of long-lasting fingerprints, the photo-cross-linking property of the Ox-Pdots has great potential for forming permanently stabilized fluorescent patterns. Latent patterns, which are readable only under UV light, are widely used in areas such as anticounterfeiting to protect banknotes, tickets, certificates, and other important documents.[34] For anticounterfeiting applications, the fluorescent patterns need to be highly resistant because they are exposed to frequent handling. We demonstrated the feasibility of the Ox-Pdots for fluorescence patterning by inkjet printing and ink stamping methods. As shown in Supporting Information Figure S5, various fluorescence patterns can be generated with the Ox-Pdots by using similar approaches demonstrated for the traditional Pdots.[34] Stability examinations were further performed by comparing the handwritten patterns of Ox-Pdots with those of oxetane-free Pdots (Figure 5). As can be seen, the photo-cross-linked patterns by the Ox-Pdots exhibit nearly permanent stability, maintaining strong fluorescence even after treatment in the most rigorous solvent THF for 10 days. In contrast, the patterns by traditional oxetane-free Pdots were severely degraded after THF treatment for a few hours. It is noted that the patterns by Ox-Pdots before photo-cross-linking also show higher stability than the traditional Pdots. It is likely that these patterns were partially cross-linked during sample preparation or strong hydrogen bonding between oxetane groups may also make a contribution. Nevertheless, these results emphasize that the photo-cross-linkable Ox-Pdots generate multicolor fluorescent patterns with an unprecedented level of stability as compared to those by traditional fluorescent inks and oxetane-free Pdots.

CONCLUSIONS

In summary, we have designed photo-cross-linkable semiconductor polymers for latent fingerprint development. Oxetanes as reactive functional groups were synthetically attached to the side-chains of fluorene-based polymers. The resulting Ox-Pdots exhibit bright multicolor fluorescence under a single-wavelength UV excitation. The high fluorescence brightness, large Stokes shift, and excellent surface properties of the Ox-Pdots result in great sensitivity and selectivity in fingerprint development as compared to those of traditional Pdots. We demonstrate high-resolution fluorescence imaging of latent fingerprints on various substrates by using the Ox-Pdots. Fingerprint ridge structures with the first, second, and third levels of detail were clearly resolved within minutes. More importantly, the fingerprint development by the Ox-Pdots undergoes chemical reactions under a UV irradiation, forming a covalently cross-linked polymer network with nearly permanent stability. We anticipate that the Ox-Pdots hold promise for rapid visualization of latent fingerprints and fluorescence patterning in anticounterfeiting applications.

ASSOCIATED CONTENT

ⓈSupporting Information

^{1}H NMR (CDCl$_3$) spectra, particle size characterizations by dynamic laser scattering and transmission electron microscopy, fingerprints on different surfaces and from different people, inkjet printing and handwritten patterns by using the Ox-Pdot inks. The Supporting Information is available free of charge on the ACS Publications website at DOI: 10.1021/acsami.5b03749.

AUTHOR INFORMATION

Corresponding Author
*E-mail: cwu@jlu.edu.cn. Phone: +86-431-8515-3853. Fax: +86-431-8516-8270.

Notes
The authors declare no competing financial interest.

■ REFERENCES

(1) Hazarika, P.; Russell, D. A. Advances in Fingerprint Analysis. *Angew. Chem., Int. Ed.* **2012**, *51*, 3524−3531.

(2) Ifa, D. R.; Manicke, N. E.; Dill, A. L.; Cooks, G. Latent Fingerprint Chemical Imaging by Mass Spectrometry. *Science* **2008**, *321*, 805−805.

(3) Li, K.; Qin, W. W.; Li, F.; Zhao, X. C.; Jiang, B. W.; Wang, K.; Deng, S. H.; Fan, C. H.; Li, D. Nanoplasmonic Imaging of Latent Fingerprints and Identification of Cocaine. *Angew. Chem., Int. Ed.* **2013**, *52*, 11542−11545.

(4) Sodhi, G. S.; Kaur, J. Powder Method for Detecting Latent Fingerprints: A Review. *Forensic Sci. Int.* **2001**, *120*, 172−176.

(5) He, Y. Y.; Xu, L. R.; Zhu, Y.; Wei, Q. H.; Zhang, M. Q.; Su, B. Immunological Multimetal Deposition for Rapid Visualization of Sweat Fingerprints. *Angew. Chem., Int. Ed.* **2014**, *53*, 12609−12612.

(6) Jaber, N.; Lesniewski, A.; Gabizon, H.; Shenawi, S.; Mandler, D.; Almog, J. Visualization of Latent Fingermarks by Nanotechnology: Reversed Development on PaperA Remedy to the Variation in Sweat Composition. *Angew. Chem., Int. Ed.* **2012**, *51*, 12224−12227.

(7) Fieldhouse, S. J. An Investigation into the Effects of Force Applied During Deposition on Latent Fingermarks and Inked Fingerprints Using a Variable Force Fingerprint Sampler. *J. Forensic Sci.* **2015**, *60*, 422−427.

(8) Jasuja, O. P.; Kaur, A.; Kumar, P. Fixing Latent Fingermarks Developed by Iodine Fuming: A New Method. *Forensic Sci. Int.* **2012**, *223*, E47−E52.

(9) Frick, A. A.; Busetti, F.; Cross, A.; Lewis, S. W. Aqueous Nile Blue: A Simple, Versatile and Safe Reagent for the Detection of Latent Fingermarks. *Chem. Commun.* **2014**, *50*, 3341−3343.

(10) Wang, J.; Wei, T.; Li, X. Y.; Zhang, B. H.; Wang, J. X.; Huang, C.; Yuan, Q. Near-Infrared-Light-Mediated Imaging of Latent Fingerprints Based on Molecular Recognition. *Angew. Chem., Int. Ed.* **2014**, *53*, 1616−1620.

(11) Wood, M.; Maynard, P.; Spindler, X.; Lennard, C.; Roux, C. Visualization of Latent Fingermarks Using an Aptamer-Based Reagent. *Angew. Chem., Int. Ed.* **2012**, *51*, 12272−12274.

(12) Hazarika, P.; Jickells, S. M.; Wolff, K.; Russell, D. A. Multiplexed Detection of Metabolites of Narcotic Drugs from a Single Latent Fingermark. *Anal. Chem.* **2010**, *82*, 9150−9154.

(13) Wolfheis, O. S. Nanoparticle-Enhanced Fluorescence Imaging of Latent Fingerprints Reveals Drug Abuse. *Angew. Chem., Int. Ed.* **2009**, *48*, 2268−2269.

(14) Leggett, R.; Lee-Smith, E. E.; Jickells, S. M.; Russell, D. A. "Intelligent" Fingerprinting: Simultaneous Identification of Drug Metabolites and Individuals by Using Antibody-Functionalized Nanoparticles. *Angew. Chem., Int. Ed.* **2007**, *46*, 4100−4103.

(15) Xu, L. R.; Zhou, Z. Y.; Zhang, C. Z.; He, Y. Y.; Su, B. Electrochemiluminescence Imaging of Latent Fingermarks through the Immunodetection of Secretions in Human Perspiration. *Chem. Commun.* **2014**, *50*, 9097−9100.

(16) Cai, K. Y.; Yang, R. Q.; Wang, Y. J.; Yu, X. J.; Liu, J. J. Super Fast Detection of Latent Fingerprints with Water Soluble CdTe Quantum Dots. *Forensic Sci. Int.* **2013**, *226*, 240−243.

(17) Wu, C. F.; Chiu, D. T. Highly Fluorescent Semiconducting Polymer Dots for Biology and Medicine. *Angew. Chem., Int. Ed.* **2013**, *52*, 3086−3109.

(18) Feng, L.; Zhu, C.; Yuan, H.; Liu, L.; Lv, F.; Wang, S. Conjugated Polymer Nanoparticles: Preparation, Properties, Functionalization and Biological Applications. *Chem. Soc. Rev.* **2013**, *42*, 6620−33.

(19) Feng, X. L.; Lv, F. T.; Liu, L. B.; Tang, H. W.; Xing, C. F.; Yang, Q. O.; Wang, S. Conjugated Polymer Nanoparticles for Drug Delivery and Imaging. *ACS Appl. Mater. Interfaces* **2010**, *2*, 2429−2435.

(20) Pecher, J.; Mecking, S. Nanoparticles of Conjugated Polymers. *Chem. Rev.* **2010**, *110*, 6260−6279.

(21) Kaeser, A.; Fischer, I.; Abbel, R.; Besenius, P.; Dasgupta, D.; Gillisen, M. A. J.; Portale, G.; Stevens, A. L.; Herz, L. M.; Schenning, A. P. H. J. Side Chains Control Dynamics and Self-Sorting in Fluorescent Organic Nanoparticles. *ACS Nano* **2013**, *7*, 408−416.

(22) Hou, Q.; Zhou, Q. M.; Zhang, Y.; Yang, W.; Yang, R. Q.; Cao, Y. Synthesis and Electroluminescent Properties of High-Efficiency Saturated Red Emitter Based on Copolymers from Fluorene and 4,7-Di(4-hexylthien-2-yl)-2,1,3-benzothiadiazole. *Macromolecules* **2004**, *37*, 6299−6305.

(23) Wu, C.; Bull, B.; Szymanski, C.; Christensen, K.; McNeill, J. Multicolor Conjugated Polymer Dots for Biological Fluorescence Imaging. *ACS Nano* **2008**, *2*, 2415−2423.

(24) Wu, C. F.; Jin, Y. H.; Schneider, T.; Burnham, D. R.; Smith, P. B.; Chiu, D. T. Ultrabright and Bioorthogonal Labeling of Cellular Targets Using Semiconducting Polymer Dots and Click Chemistry. *Angew. Chem., Int. Ed.* **2010**, *49*, 9436−9440.

(25) Dilag, J.; Kobus, H.; Ellis, A. V. CdS/Polymer Nanocomposites Synthesized via Surface Initiated RAFT Polymerization for the Fluorescent Detection of Latent Fingermarks. *Forensic Sci. Int.* **2013**, *228*, 105−114.

(26) Fernee, M. J.; Tamarat, P.; Lounis, B. Cryogenic Single-Nanocrystal Spectroscopy: Reading the Spectral Fingerprint of Individual CdSe Quantum Dots. *J. Phys. Chem. Lett.* **2013**, *4*, 609−618.

(27) Algarra, M.; Radotic, K.; Kalauzi, A.; Mutavdzic, D.; Savic, A.; Jimenez-Jimenez, J.; Rodriguez-Castellon, E.; da Silva, J. C. G. E.; Guerrero-Gonzalez, J. J. Fingerprint Detection and Using Intercalated CdSe Nanoparticles on Non-Porous Surfaces. *Anal. Chim. Acta* **2014**, *812*, 228−235.

(28) Gao, F.; Lv, C. F.; Han, J. X.; Li, X. Y.; Wang, Q.; Zhang, J.; Chen, C.; Li, Q.; Sun, X. F.; Zheng, J. C.; Bao, L. R.; Li, X. CdTe-Montmorillonite Nanocomposites: Control Synthesis, UV Radiation-Dependent Photoluminescence, and Enhanced Latent Fingerprint Detection. *J. Phys. Chem. C* **2011**, *115*, 21574−21583.

(29) Wu, C. F.; Schneider, T.; Zeigler, M.; Yu, J. B.; Schiro, P. G.; Burnham, D. R.; McNeill, J. D.; Chiu, D. T. Bioconjugation of Ultrabright Semiconducting Polymer Dots for Specific Cellular Targeting. *J. Am. Chem. Soc.* **2010**, *132*, 15410−15417.

(30) Hartzell-Baguley, B.; Hipp, R. E.; Morgan, N. R.; Morgan, S. L. Chemical Composition of Latent Fingerprints by Gas Chromatography-Mass Spectrometry - An Experiment for an Instrumental Analysis Course. *J. Chem. Educ.* **2007**, *84*, 689−691.

(31) Muller, C. D.; Falcou, A.; Reckefuss, N.; Rojahn, M.; Wiederhirn, V.; Rudati, P.; Frohne, H.; Nuyken, O.; Becker, H.; Meerholz, K. Multi-Colour Organic Light-Emitting Displays by Solution Processing. *Nature* **2003**, *421*, 829−833.

(32) Muller, D.; Gross, M.; Meerholz, K.; Braig, T.; Bayerl, M. S.; Bielefeldt, F.; Nuyken, O. Novel Cross-Linkable Hole-Transport Monomer for Use in Organic Light Emitting Diodes. *Synth. Met.* **2000**, *111*, 31−34.

(33) Holder, E. H.; Robinson, L. O.; Laub, J. H. *The Fingerprint Sourcebook*; U.S. Department of Justice, Office of Justice Programs, National Institute of Justice: Washington, DC, 2011; Chapter 9, pp 9-1−9-26.

(34) Chang, K. W.; Liu, Z. H.; Chen, H. B.; Sheng, L.; Zhang, S. X. A.; Chiu, D. T.; Yin, S. Y.; Wu, C. F.; Qin, W. P. Conjugated Polymer Dots for Ultra-Stable Full-Color Fluorescence Patterning. *Small* **2014**, *10*, 4270−4275.